

## Synthesis and characterization of Cu doped NiO nanoparticles

B. Ramasubba Reddy<sup>1</sup>, G. S. Harish<sup>2</sup>, Ch. Seshendra Reddy<sup>3</sup>,  
P. Sreedhara Reddy<sup>4</sup>

<sup>1, 2, 3, 4</sup> Department of Physics, Sri Venkateswara University, Tirupati, 517502, India

**Abstract:** Copper doped NiO nanoparticles were synthesized by chemical precipitation method and studied the structural, compositional, morphological, luminescence and optical properties using X-ray diffraction (XRD), Energy dispersive analysis of X-rays (EDAX), Scanning electron microscopy (SEM), PL Fluorimeter and High Resolution Raman spectroscopy. XRD studies confirm the fcc structure of the prepared samples. EDAX showed the effective doping of copper into NiO. For pure NiO, PL peak was observed at 434 nm and an enhancement in the PL intensity was observed with increasing dopant concentration. The Raman peak observed at 518 cm<sup>-1</sup> confirms the Ni-O bonds and no impurity peaks were observed due to dopant.

**Keywords:** Cu-doped NiO, XRD, RAMAN, EDAX

### I. Introduction

At present, nano-sized materials have attracted much attention because of their unusual properties based on size-quantization effect and large surface area [1 - 3]. Nanosized nickel -oxide (NiO) is of great interest because it exhibits particular catalytic [4, 5], anomalous electronic [6- 8], and magnetic [9– 12] properties. NiO, as one of the relatively few metal oxides which exhibits p-type conductivity. It is a stable wide band gap material and can be used as a transparent p-type semiconducting layer. Among transition metal oxides, nickel oxide (NiO) has been received considerable attention due to their wide range of applications in various fields, including catalysis [4, 5], electrochromic windows [13], and sensors [14]. The characteristic properties of nanosized NiO particles also enable to tailor the properties for a variety of applications. In the present study, pure and copper doped NiO nanoparticles were synthesized using chemical co-precipitation method and studied various properties like structural, compositional, morphological, luminescence and Raman studies.

### II. Experimental details

All chemicals were of analytical reagent grade and were used without further purification. Pure and Cu doped NiO nanoparticles were prepared by chemical precipitation method. The reactants were NiCl<sub>2</sub>·6H<sub>2</sub>O and CuSO<sub>4</sub>·5H<sub>2</sub>O. Ultrapure de-ionized water was used as the reaction medium in all the synthesis steps. In a typical synthesis, desired molar proportions of NiCl<sub>2</sub>·6H<sub>2</sub>O and CuSO<sub>4</sub>·5H<sub>2</sub>O (0, 2, 4 and 6 at.%) each in 100 ml were dissolved in ultrapure de-ionized water and stirred for 30 minutes, NaOH solution was drop wisely added to the solution to adjust the pH value to 10. Stirring was continued for four hours to get fine precipitation. The obtained precipitate was washed with de-ionized water for several times. Finally, the powders were vacuum dried for 3 hours at 80 °C to obtain pure and Cu doped NiO nanoparticles.

### III. Characterization

The X-ray diffraction patterns of the samples were collected on a Rigaku D X-ray diffractometer with the Cu-K $\alpha$  radiation ( $\lambda=1.5406\text{\AA}$ ). Morphology and elemental composition of the prepared samples were analyzed through EDAX using Oxford Inca Penta FeTX3 EDS instrument attached to Carl Zeiss EVO MA 15 scanning electron microscope. Photoluminescence spectra were recorded in the wavelength range of 400–600 nm using PTI (Photon Technology International) Fluorimeter with a Xe-arc lamp of power 60 W and an excitation wavelength of 320 nm was used. Raman Spectroscopic studies of the as prepared samples were carried out using LabRam HR800 Raman Spectrometer.

### IV. Results and discussion

#### 4.1. Structural analysis by X-ray diffraction (XRD)

The X-ray diffraction patterns for the Pure NiO and Cu doped nanoparticles are shown in Fig. 1. From the figure it is obvious that the peaks are indexed as (111), (200), (220), (311) and (222) planes at  $2\theta$  values 37.39°, 43.45°, 62.98°, 75.5° and 79.49° that correspond to face centered cubic structure of NiO nanoparticles which are in consistent with the JCPDS (No. 47-1049) data.

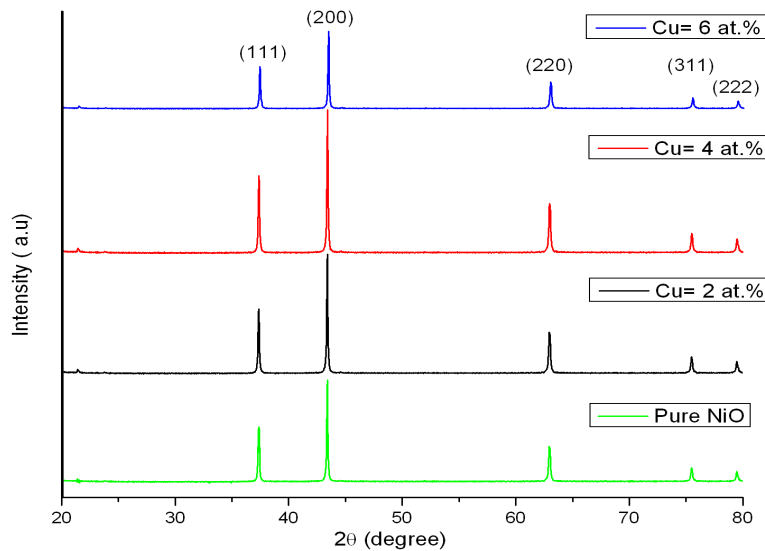


Fig.1. XRD patterns of Pure and Cu doped NiO nanoparticles

The average particle size of Pure and Cu doped NiO nanoparticles was calculated using Debye–Scherrer’s equation [a] by determining the width of the (200) Bragg’s reflection.

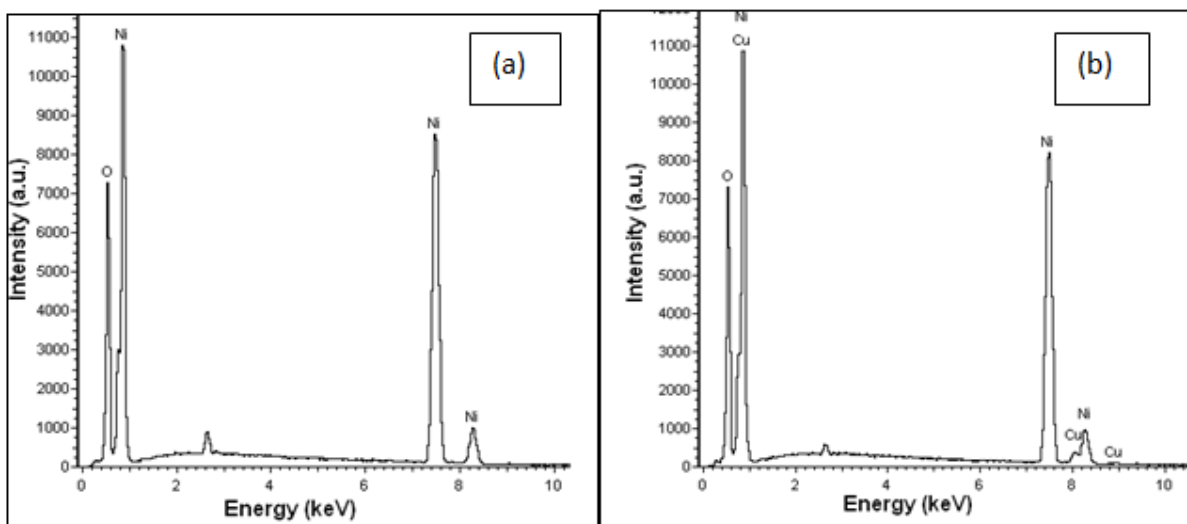
$$D = \frac{0.94\lambda}{\beta_{hkl} \cos \theta}$$

Where, D is the average particle size and  $\beta_{hkl}$  is full width at half maximum of XRD peak expressed in radians and  $\theta$  is the position of the diffraction peak.

The average sizes of the particles prepared at different concentration of Pure NiO and Cu ( 2, 4 and 6 at.%) doped NiO nanoparticles were of 76, 64, 52 and 60 nm, respectively hence the decrease in particle size with increasing doping concentration has predicted. Increase in particle size of Cu (6%) doped NiO nanoparticles, may be due to interactions between neighboring Cu-Cu ions.

#### 4.2. Compositional analysis

The EDAX profile of prepared Pure and Cu (2, 4 and 6 at %) doped NiO nanoparticles are shown in Fig.2. It is evident from the EDAX Spectra, no other elemental peaks other than Ni, O and Cu are observed except that only the elemental carbon arises due to adhesion of carbon tape on to the stud used in the analysis. The results confirm the effective doping of Cu into NiO.



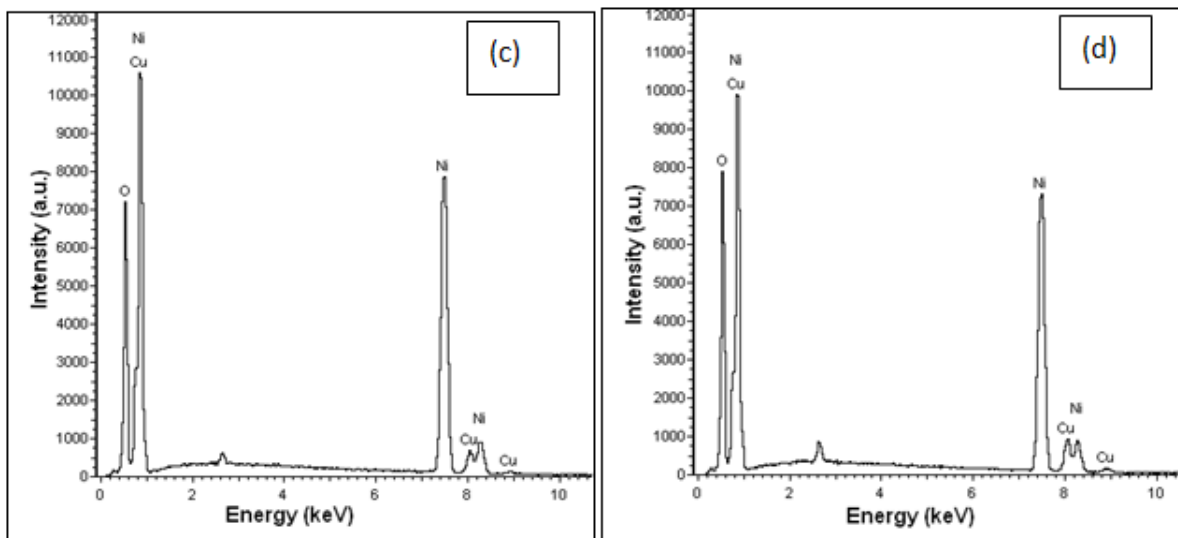


Fig. 2. Representative EDS spectrum of prepared nanoparticles (a) Pure NiO, (b) Cu (2 at.%), (c) Cu (4 at.%) and (d) Cu (6 at.%)

### 4.3. Morphological studies

The size and morphology of the Pure and Cu doped NiO nanoparticles were observed by SEM measurements. The SEM images of Pure and Cu(2, 4 and 6 at.%) doped NiO nanoparticles were shown in Fig. 3(a), 3(b), 3(c) and 3(d) respectively.

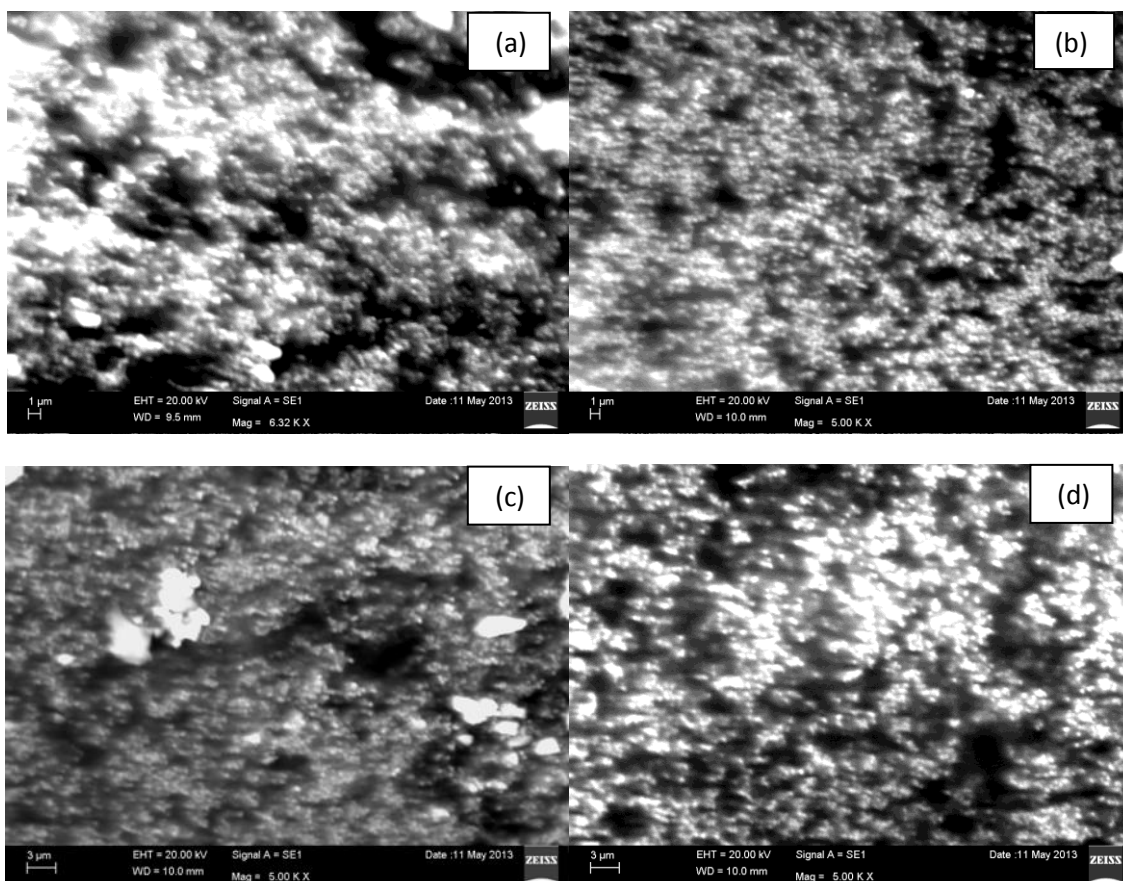


Fig. 3. SEM images of (a) Pure NiO and (b) Cu( 2 at. %), (c) Cu(4 at.%) and (d) Cu( 6 at.%) doped NiO nanoparticles

The prepared NiO nanoparticles are more or less spherical and were found to be homogeneous and the particles are almost isolated with no substantial aggregation.

#### 4.4. Photo Luminescence

Fig. 4 shows the PL spectra of Pure and Cu doped NiO nanoparticles under 320 nm wavelength excitation at room temperature. The NiO sample with a higher crystallinity and a larger particle size shows a stronger band-band PL emission at 434 nm.

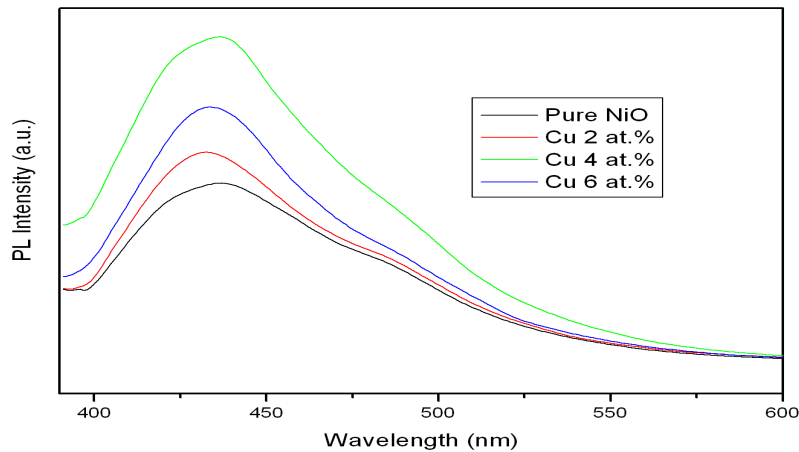


Fig.4. PL spectra of (a) Pure NiO and (b) Cu( 2 at. %), (c) Cu(4 at.%) and (d) Cu( 6 at.%) doped NiO nanoparticles

The stronger the band-band PL intensity of NiO nanoparticles, the higher the recombination rate of photoinduced electron-hole pair. The deeply trapped holes are more or less localized at deep traps, exhibit a lower oxidizing potential, and prefer to react with physically adsorbed substances [15, 16]. Heat treatment may result in a slight deviation from NiO stoichiometry and the cation vacancy and/or interstitial oxygen trapping in the NiO lattice leads to two shoulder peaks at 496 and 540 nm in green emission band confirmed presence of such defects in NiO lattice. Nickel vacancies can be produced due to the charge transfer between  $Ni^{2+}$  and  $Ni^{3+}$  [17]. As seen in Fig. 4, all the samples showed excitonic PL emission band at 2.86 eV (434 nm) resulting from the surface oxygen vacancies of NiO samples [18]. Blue emissions in PL spectrum with a strong band centered at 434 nm confirmed the presence of Cu doped NiO nanoparticles and no impurity peaks were observed [19]. PL intensity is enhanced with increasing dopant concentration and decreased for 6 at.% of Cu, because of the increment in the particle size.

#### 4.5. Raman studies

Fig.5 shows the Raman spectra of Pure and Cu doped NiO nanoparticles. The Raman spectrum exhibited a strong, broad peak at  $518\text{ cm}^{-1}$  due to the Ni-O stretching mode [20, 21]. From fig.5, it is clear that, no impurity peaks were observed and with increasing dopant concentration, the broad peak centered at  $518\text{ cm}^{-1}$  shifted towards the higher wavelength side.

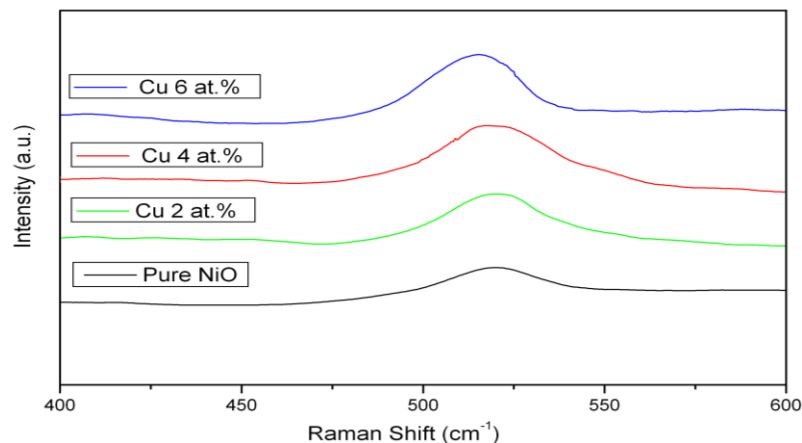


Fig.5. Raman spectra of (a) Pure NiO and (b) Cu( 2 at. %), (c) Cu(4 at.%) and (d) Cu( 6 at.%) doped NiO nanoparticles

## V. Conclusions

Pure and Cu doped NiO nanoparticles were prepared by chemical precipitation method using NiCl<sub>2</sub>·6H<sub>2</sub>O and CuSO<sub>4</sub>·5H<sub>2</sub>O as reactants. Structural, compositional, morphological, Luminescence and optical properties of the prepared samples were studied using X-ray diffraction, Energy dispersive spectroscopy, scanning electron microscopy (SEM), PTI Fluorimeter and High Resolution Raman spectroscopy. XRD studies confirmed the fcc structure of the prepared samples. EDAX spectra showed the effective doping of copper into NiO. For pure NiO, PL peak was observed at 434 nm and an enhancement in the PL intensity was observed with increasing Copper concentration. The Raman peak observed at 518 cm<sup>-1</sup> confirms the Ni-O bonds and no impurity peaks were observed due to dopant incorporation.

## REFERENCES

- [1.] K.J. Klabunde, J. Stark, O. Koper, C. Mohs, G.P. Dong, S. Decker, Y. Jiang, I. Lagadic, D. Zhang, *J. Phys. Chem.* 100 (1996) 12142–12153.
- [2.] P.V. Kamat, *Chem. Rev.* 93 (1993) 267–300.
- [3.] B.G. Ershov, E. Janata, A. Henglein, *J. Phys. Chem.* 97 (1993) 339–343.
- [4.] A. Alejandre, F. Medina, P. Salagre, A. Fabregat, J.E. Sueiras, *Appl. Catal. B: Environ.* 18 (1998) 307–315.
- [5.] C.L. Carnes, K.J. Klabunde, *J. Mol. Catal. A: Chem.* 194 (2003) 227–236.
- [6.] L. Soriano, M. Abbate, J. Vogel, J.C. Fuggle *Chem. Phys. Lett.* 208 (1993) 460–464.
- [7.] D. Alders, F.C. Voogt, T. Hibma, G.A. Sawatzky, *Phys. Rev. B* 54 (1996) 7716–7719.
- [8.] V. Biju, M.A. Khadar, *Mater. Sci. Eng. A* 304–306 (2001) 814–817.
- [9.] S.A. Makhlof, F.T. Parker, F.E. Spada, A.E. Berkowitz, *J. Appl. Phys.* 81 (1997) 5561–5563.
- [10.] R.H. Kodama, S.A. Makhlof, A.E. Berkowitz *Phys. Rev. Lett.* 79 (1997) 1393–1396.
- [11.] R.H. Kodama, *J. Magn. Magn. Mater.* 200 (1999) 359–372.
- [12.] F. Bodker, M.F. Hansen, C.B. Koch, S.J. Morup, *J. Magn. Magn. Mater.* 221 (2000) 32–36.
- [13.] D. Das, M. Pal, E.D. Bartolomeo, E. Traversa, D. Chakravorty, *J. Appl. Phys.* 88 (2000) 6856–6860.
- [14.] Y. Wang, J. Zhu, X. Yang, L. Lu, X. Wang, *Thermochim. Acta* 437 (2005) 106–109.
- [15.] D.W. Bahnemann, M. Hilgendorff, R. Memming, *J. Phys. Chem. B*, 101 (1997) 4265–4275.
- [16.] Y. Tamaki, A. Furube, M. Murai, K. Hara, R. Katoh, M. Tachiya, *J. Amer. Chem. Soc.* 128 (2006) 416–417.
- [17.] S. Mochizuki, T. Saito *Physica B* 404 (2009) 4850–4853.
- [18.] M.H. Zhou, J.G. Yu, S.W. Liu, P.C. Zhai, L. Jiang, *J. Hazard. Mater.* 154 (2008) 1141–1148.
- [19.] S. Mohseni Meybodi, S.A. Hosseini, M. Rezaee, S.K. Sadrnezhad, D. Mohammadyan, *Ultrason. Sonochem.* 19 (2012) 841–845.
- [20.] S.I. Cordoba-Torresi, A. Hugot-Le Goff, S. Joiret, *J. Electrochem. Soc.* 138 (1991) 1554.
- [21.] N. Dharmaraj, P. Prabu, S. Nagarajan, C.H. Kim, J.H. Park, H.Y. Kim, *Mater. Sci. Eng., B* 128 (2006) 111–114.